ELSEVIER

Thermochimica Acta 303 (1997) 171–181

thermochimica acta

Thermochemistry of manganese oxides in reactive gas atmospheres: Probing redox compositions in the decomposition course $MnO_2 \rightarrow MnO$

M.I. Zaki*, M.A. Hasan, L. Pasupulety, K. Kumari

Chemistry Department, Faculty of Science, University of Kuwait, P.O. Box 5969 Safat, 13060, Kuwait

Received 17 January 1997; received in revised form 11 June 1997; accepted 29 June 1997

Abstract

The thermal decomposition course $MnO_2 \rightarrow MnO$ was examined in various gas atmospheres (O_2, air, N_2 and H_2) by temperature-programmed studies employing thermogravimetry and differential thermal analysis. Weight-invariant thermal events encountered were subjected to non-isothermal and isothermal kinetic analysis. Product analysis was carried out using infrared spectroscopy and X-ray diffractometry. Cyclic TG experiments carried out in air have revealed that, of the intermediate decomposition products characterized, viz. Mn_5O_8, Mn_2O_3 Mn_3O_4, the mixed-valence Mn_3O_4 ($= Mn(II)Mn_2(III)O_4$) can tolerate reversible oxygenation–deoxygenation processes at (500–1050°C). Moreover, the presence of Mn(II) in the mixed-valence Mn_5O_8 ($= Mn_2(II)Mn_3(IV)O_8$) is seen to sustain a synproportionation of Mn(II)/Mn(IV) during the oxide deoxygenation, giving rise to Mn(III) species ($= Mn_2O_3$). The electron-mobile environment thus established in such mixed-valence oxides is seen to promise a catalytic potential in oxidation/reduction reactions.

Keywords: Manganese oxides; Redox MnO_x compositions; Thermal decomposition of MnO_2; Thermochemistry; Thermochemistry of manganese oxides

1. Introduction

The title 'redox' is meant to refer to metal oxide compositions (MO_x) that can tolerate bulk oxygenation–deoxygenation in a reversible fashion and, consequently, have their metal ions oxidized and reduced. This means that, for the present work, processes leading to a mere generation of point defects (MO_{x+y} and MO_{x-y}, respectively) in the oxide lattice are excluded. Accordingly, redox compositions of MO_x are those described by Zener [1] as being capable of mobilizing electrons and, thus, generating the mobile-electron environment required by redox catalysis [2]. The present study is, in fact, a part of a comprehensive investigation that explores candidate metal oxides for the chemical makeup of deep oxidation catalysts [3,4] urged by environmental necessities [5].

Within the present test MnO_x systems, MnO_2 was among the oldest examined metal oxide catalyst [6] and found to possess a potential activity in redox reactions. Its existence only tolerates a narrow range of non-stoichiometry: $MnO_{2-1.9}$ [7]. Thus, heating β-MnO_2 at 500–1100°C in air has been found to trigger its decomposition into a number of lower oxides:

*Corresponding author. Tel.: 965 4811188/5606; fax: 965 4816482; e-mail: zaki@kuc01.kuniv.edu.kw

0040-6031/97/$17.00
PII S0040-6031(97)00258-X

MnO_x, with $1 \leq x \leq 1.6$ [8]. Recent temperature-programmed studies [9] of the decomposition course of Mn(II)-oxysalts have disclosed high sensitivity of the manganese oxidation state to the surrounding environment of oxyanions and gas phase being released.

Hence, the present investigation was designed to characterize MnO_x compositions formed throughout the thermal decomposition course of MnO_2 in O_2, air, N_2 and H_2 dynamic atmospheres, by means of thermogravimetry, infrared spectroscopy and X-ray powder diffractometry. Non-isothermal and isothermal kinetic parameters of the thermochemical events involved were derived from TG curves obtained as a function of heating rate. Finally, redox compositions were probed by means of a set of cyclic thermogravimetry experiments carried out on test samples in a dynamic atmosphere of air.

2. Experimental

2.1. Materials

MnO_2 (β-form, pyrolusite-like) was a 99.9% pure product of Fluka (Switzerland). It was calcined by heating in a stream of air at 630°, 700°, and 850° and 1100°C for 2 h. The temperatures applied were chosen on the basis of thermal analysis results (vide infra). The calcination products are indicated by the calcination temperature applied; thus, $MnO_2(630)$ refers to the calcination product at 630°C.

For reference purposes, AR-grade Mn_2O_3, Mn_3O_4 and MnO were obtained from Aldrich (USA), whereas Mn_5O_8 was prepared by calcination of synthetic $MnC_2O_4 \cdot 2H_2O$ at 300°C for 3 h [9,10]. These model oxides were kept dry, together with MnO_2 and its calcination products, over silica gel in a vacuum desiccator until further use.

Gases used to provide the atmosphere for thermal analysis were 99.999% pure N_2, O_2 and H_2. These were products of Kuwait Oxygen and Acetylene (KOAC).

2.2. Thermal analysis

Thermogravimetry (TG) and differential thermal analysis (DTA) were performed using automatic TGA-50 and TGD-50 Shimadzu analyzers (Japan) respectively, equipped with on-line TA-50WS work station for data acquisition and handling. DTA curves were recorded while heating test samples ($\simeq$ 20 mg) up to 1100°C at an invariable heating rate ($\phi = 10$°C/min) and in a dynamic atmosphere of air (30 ml/min); the thermally inert reference material was α-Al_2O_3 (Shimadzu).

TG curves were obtained by cyclic and non-cyclic thermogravimetry of ~20 mg portions of test samples. The non-cyclic TG was carried out by heating test sample at an invariable heating rate ($\phi = 10$°C/min) in different dynamic gas atmospheres (air, N_2, O_2 and H_2 at 30 ml/min), and at variable heating rates ($\phi = 10$, 15 and 30°C/min) in a dynamic atmosphere of air, up to 1100°C. Non-isothermal and isothermal kinetic parameters (namely, reaction activation energy (ΔE), order (n), frequency factor (A), and rate constant (k)) of weight loss (WL) processes monitored in the TG curves of MnO_2 in air were determined by means of an automatic data treatment in the work station, implementing the mathematical apparatus of Ozawa's method [11]:

$$\log \phi_1 + 0.4567(\Delta E/RT_1) = \log \phi_2 + 0.4567(\Delta E/RT_2) = \cdots,$$

(for determination of ΔE from the slope of $\log \phi - 1/T$ plots)

$$G(x) \equiv A\theta = (1/n - 1)[(1 - x)^{1-n} - 1],$$

where x is the fraction of reaction completed, and θ the reduced time at x *(for determination of n and A)*.

$$t = \theta \exp(\Delta E/RT),$$

where t is the reaction time required to reach the weight loss at θ when a constant temperature is maintained *(for construction of isothermal $x - t$ plots)*.

$$k = A \exp(-\Delta E/RT).$$

(for determination of k by substitution for T at given A and ΔE values).

The cyclic TG was conducted by heating at an invariable rate (10°C/min) to a given temperature (T_2) followed by cooling at the same rate to a lower temperature (T_1). The heating–cooling cycle (denoted as cycle-1) was carried out twice in succession. Then, cycle-2 (between T_1 and T_3), cycle-3 (between T_1 and T_4) and cycle-4 (between T_1 and T_5) were carried out

(where $T_5 > T_4 > T_3 > T_2$), using a fresh portion of the same test sample for each cycle. Cyclic TG was meant to probe reversibility of weight-change processes encountered. Thus, temperature ranges of measurements (cycle) are dependent on material tested.

2.3. Spectroscopic analysis

X-ray powder diffractormetry (XRD) was carried out at room temperature, using a Siemens D5000 diffractometer (Germany) equipped with a Ni-filtered CuK_α radiation ($\lambda = 1.5418$ Å; 40 kV, 30 mA), in the 2θ range between 10° and 80°, with a divergence slit of 1°. An on-line microcomputer facilitated data acquisition and handling. For phase identification purposes, automatic JCPDS library search (standard SEARCH software) and match (standard DIFFRAC AT software) were employed.

Infrared absorption (IR) spectra were taken from KBr-supported test samples (< 1 wt%), over the frequency range 4000–400 cm^{-1}, at a resolution of 4 cm^{-1}, using a model 2000 Perkin–Elmer FT spectrophotometer (UK). An on-line data station facilitated spectra acquisition and handling.

3. Results and discussion

3.1. Characterization of MnO_2 decomposition course

3.1.1. Decomposition events

Fig. 1 displays TG curves obtained for MnO_2 in various atmospheres. The curves obtained in O_2, air and N_2 exhibit generally similar thermal behaviours, monitoring three major events: (I) WL-process (7.5–8.25%), T_{max} = 680–650°C; (II) WL-process (~ 1%), T_{max} = 830–820°C; and (III) WL-process (2.5–3.6%), T_{max} = 1050–880°C. Corresponding DTA curves (not shown) revealed that WL-processes involved in the events (I) and (III) are evidently endothermic. It is obvious from Fig. 1, that in O_2-rich atmosphere, event (I) is slightly retarded ($T_{max} = 650(N_2) \rightarrow 680°C(O_2)$), but event-III is considerably retarded ($T_{max} = 880(N_2) \rightarrow 1050°C(O_2)$). This may account for a reversible behaviour for the WL-processes involved, particularly in event (III). It is worth noting that the appreciable acceleration conceded by event (III) in the absence of O_2 (i.e. in N_2) resulted in its strong overlap with event (II), making the latter much less visible in the TG curve obtained in N_2 than the curves obtained in air and O_2.

Molecular stoichiometry calculations based on the WL magnitudes determined in the TG curves help speculating about the nature of the decomposition reactions involved. Accordingly, event (I) is thought to involve deoxygenation of MnO_2 to the onset of formation of $MnO_{1.6}$ ($\simeq Mn_5O_8$). The closer agreement between the observed (7.5%) and calculated (7.4%) WL values in O_2 than in the case of N_2 (obs. 8.25%) emphasizes the importance of oxygen-rich atmosphere for the thermal genesis of the suggested manganoxide ($Mn_5O_8 = Mn_2(II)Mn_3(IV)O_8$) in a state of high purity. As a matter of fact, the literature documents but a few reports detecting formation of pure manganoxide from MnO_2 as a precursor compound [8,12]. In contrast, precursor compounds based on Mn^{II}, such as manganous oxalate [9,10], citrate [13], carbonate [14] and oxide [15], are frequently applied to obtain Mn_5O_8 by heating in air (or in a mixed stream of $O_2 + N_2$).

Molecular stoichiometry calculations predict, moreover, that the WL ($\simeq$ 1.0%) accompanying event (II) is very close to that expected (0.8%) for a further deoxygenation of $MnO_{1.6}$ down to $MnO_{1.5}$ ($\simeq Mn_2O_3$). In O_2-rich atmosphere, the product appears to be rather stable up to heating to near 1050°C. In N_2, however, the product of event (II) seems to decompose immediately (T_{max} = 880°C) via event (III) giving rise to a thermally stable MnO_x composition. The WL pertaining to event (III) (2.5–3.6%) is in close agreement with that expected (3.4%) for the deoxygenation of $MnO_{1.5}$ to produce $MnO_{1.3}$ ($\simeq Mn_3O_4$). The obvious sensitivity of the operational range of temperature of event (III) to the availability of oxygen in the surrounding gas atmosphere (Fig. 1) may account for a strongly reversible $MnO_{1.5} \rightarrow MnO_{1.3} + 0.2O$ process (i.e. $3Mn_2O_3 \rightleftarrows 2Mn_3O_4 + \frac{1}{2}O_2$). Fig. 1 also shows that pure $MnO_{1.28-1.35}$ (Mn_3O_4) is obtainable in N_2 atmosphere, whereas in O_2 and air the WL determined (< 3.6%) accounts for the formation of excess oxygen containing product (Mn_3O_{4+x}).

The TG curve obtained in H_2 atmosphere (Fig. 1) monitors a significantly different thermal behaviour for MnO_2, by displaying a single, strong WL-process (event (IV)) succeeded by a strictly weight-invariant

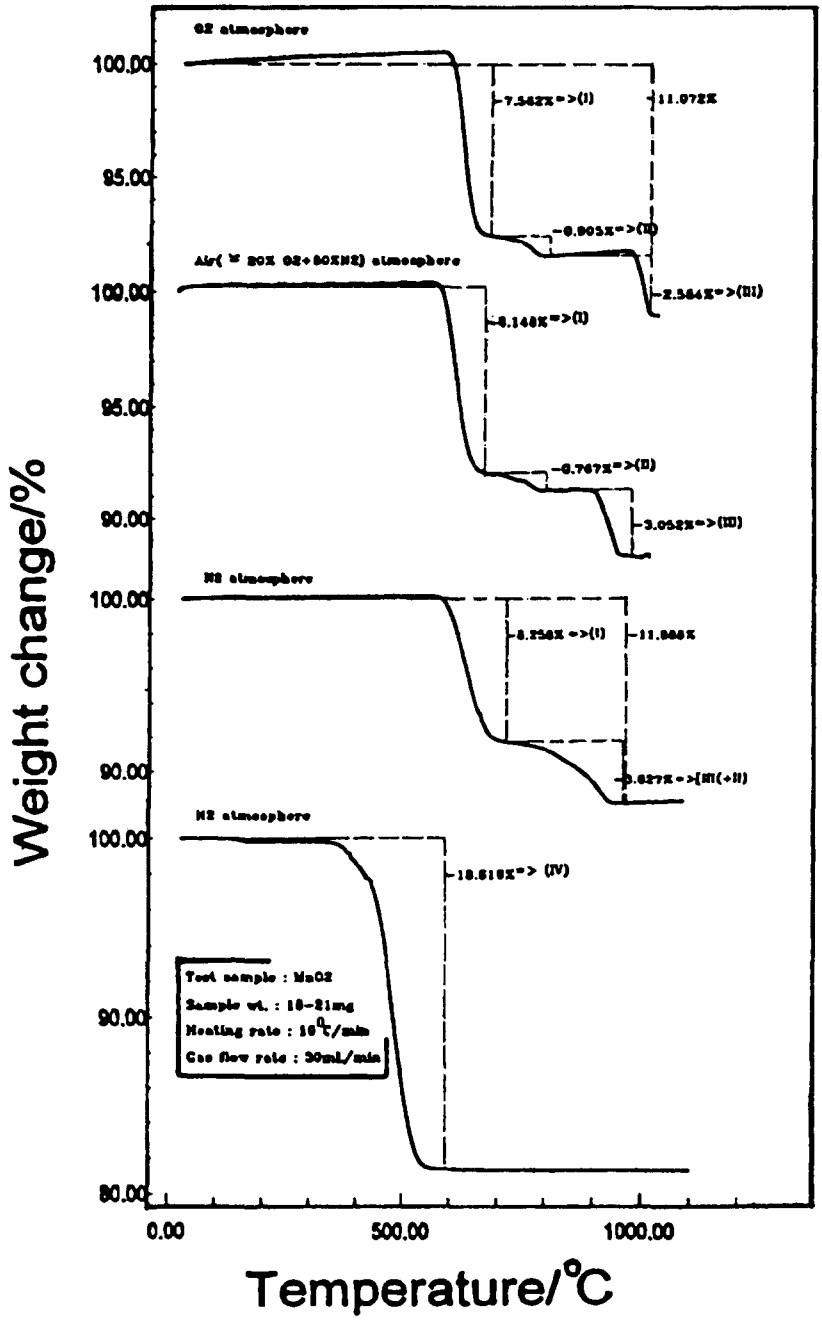

Fig. 1. TG curves obtained for MnO_2 in the various gas atmospheres indicated.

behaviour. The occurrence of event (IV) is shown to maximize at an appreciably lower temperature (namely at $T_{max} = 480°C$) than event (I) ($T_{max} = 680–650°C$). Hence, one can justifiably consider the WL-process involved in event (IV) as being chemically-driven under the reductive influence of the H_2 atmosphere. The WL determined (18.6%) is almost identical to that (18.4%) expected for the reduction of

MnO_2 down to MnO, which remains quite stable to further heating up to 1100°C (Fig. 1). It is obvious that intermediate compositions in the range MnO_2–MnO are unstable to heating in H_2 at the operational temperature range of event (IV), i.e. at 350–500°C.

3.1.2. Decomposition products

Decomposition of MnO_2 was ex-situ effected by heating in air for 2 h at temperatures specified by the corresponding TG curve (Fig. 1). Products, thus obtained, were examined by XRD and IR. The results were compared with signature XRD and IR spectra exhibited by model Mn-oxides, viz. Mn_5O_8, Mn_2O_3, Mn_3O_4 and MnO, for identification purposes. Outcome of the product analysis is summarized in Table 1.

Accordingly, MnO_2 ($Mn(IV)O_2$), pyrolusite-like β-structured, is deoxygenated via event (I) ($T_{max} = 680$°C) to produce a largely non-crystalline material, the composition of which corresponds, according to TG- and IR-data (Table 1), to that of the oxide phase Mn_5O_8 ($Mn_2(II)Mn_3(IV)O_8$). A further deoxygenation via event (II) ($T_{max} = 830$°C) leads to conversion of the manganoxide into bixbyite-like α-Mn_2O_3 ($Mn_2(II)O_3$). The product is quite stable in O_2-rich atmosphere till 1050°C, where event (III) enforces a further deoxygenation transforming α-Mn_2O_3 into Hausmannite-like Mn_3O_4 ($Mn(II)\ Mn_2(III)O_4$).

Table 1 shows that when β-MnO_2 is heated in H_2, event (IV) ($T_{max} = 480$°C) occurs and results in the formation of a manganosite-like MnO (Mn(II)O). No stable intermediate MnO_x composition is detectable (Fig. 1), and the eventual product is shown to be quite stable to further heating in H_2 up to 1100°C.

3.1.3. Kinetic parameters

Non-isothermal and isothermal kinetic parameters for thermal events (namely, I and III) exhibited by MnO_2 in air were derived from TG curves obtained as a function of heating rate ($\phi = 10°$, 15°, 20° and 30°C/min) [11]. The corresponding set of graphical correlations for event (I) (Fig. 1) are illustrated in Fig. 2. A similar set was constructed for event (III) (not shown). However, it was practically impossible to analyze event (II), since it became rather irresolvable at $\phi > 15$°C/min. Thus, Table 2 summarizes kinetic parameters calculated for events I and III only.

It is obvious from Table 2 that the reaction involved in event (I), $5MnO_2 \rightarrow Mn_5O_8 + O_2$, approximates first-order kinetics and requires an activation energy of 49.86 kcal/mol (= 208.72 kJ/mol). On the other hand, the reaction involved in event (III), $3Mn_2O_3 \rightarrow 2Mn_3O_4 + \frac{1}{2}O_2$, assumes a lower order ($n = 0.6$) and a much higher activation energy ($\Delta E = 128.5$ kcal/mol). This can well be correlated with the observed (Fig. 1) stronger control of the availability of oxygen in the surrounding atmosphere on the kinetics of event (III) than event (I). Fig. 1 indicates consistently that the higher the amount of oxygen (i.e. the higher the partial pressure of oxygen) in the surrounding atmosphere the stronger the retardation to the deoxygenation of Mn_2O_3 into Mn_3O_4. This may emphasize the stronger reversibility of event (III) than event (I).

3.2. Probing of redox MnO_x compositions

In order to allocate the redox among the MnO_x compositions encountered in the decomposition course of manganese dioxide, i.e. among MnO_2, $MnO_{1.6}$ (= Mn_5O_8), $MnO_{1.5}$ (= Mn_2O_3), $MnO_{1.3}$ (= Mn_3O_4) and MnO, cyclic TG experiments were performed on MnO_2 in the atmosphere of air. The principle goal was to indicate MnO_x compositions that can tolerate deoxygenation–oxygenation cycles in a reversible fashion. TG curves thus obtained are exhibited in Fig. 3. The results convey that none of the MnO_x compositions encountered during MnO_2 decomposition in air can be described as redox, except for Mn_3O_4. Mn_3O_4 is formed during the heating half of first cycle-4 (ambient temperature → 1050°C), and remained weight-invariant during the subsequent cooling half (1050° → 500°C). During the heating half of the second cycle-4 (500° → 1050°C), it initially gains weight (2.9%) and, eventually, loses the weight gained at 1000° → 1050°C. A subsequent third cycle-4 (not show) was accompanied by identical weight gain and loss magnitudes and processes. Similar cyclic TG results were observed in pure O_2 atmosphere; however, in pure N_2 no weight gain was detected. Thus, the weight gain is evidently due to oxygen uptake, and the amount gained (2.9%) is very close to that (2.8%) lost during the deoxygenation of Mn_2O_3 to give Mn_3O_4 at $T_{max} = 1050$°C (Fig. 1).

Table 1
Observed and reference IR and XRD analyses results for MnO_2 and its decomposition products, MnO_2 (T), in air and hydrogen ($MnO_2(T)H$) atmospheres. Heating temperatures, (T), were chosen on basis of corresponding TG results (see Fig. 1)

Test sample	IR results				XRD results					Conclusion
	observed		reference		observed		reference			
	absorption ν/cm^{-1}	line shape [a]	absorption ν/cm^{-1}	material	$d/Å$	I/I°	$d/Å$	I/I°	material	
MnO_2	407	m, sp	405	β-MnO_2, Ref. [16]	3.088	100	3.105	100	β-MnO_2; Pyrolusite;	consists solely of Pyrolusite-like β-MnO_2, which assumes a tetragonal structure
	555	vs	545		1.563	12	1.552	10	JCPDS: 24-0735	
	681	s	675		2.205	10	2.197	9		
	715	w, sh	710							
MnO_2 (630)	419	vw, sp	419(i)	(i) present Mn_2O_3 and	2.709	100	2.713	100	α-Mn_2O_3; Bixbyite;	consists of a non-crystalline material having the composition of Mn_5O_8 ($Mn_2(II)Mn_3(IV)O_8$) as a major component, and crystalline Bixbyite-like α-Mn_2O_3 as a minor component
	424	w, sh	424(ii)	α-Mn_2O_3, Ref. [17]	1.668	24	1.663	22	JCPDS: 31-0825	
	510	s, sh	509(ii)		3.840	16	3.837	15		
	519	vs	526(i)	(ii) present Mn_5O_8						
	573	vs	573(i)							
	602	s, sh	607(ii)							
	667	m, sh	668(i)							
MnO_2 (700)	424	w, sh	424(i)	(i) and (ii) as above	2.716	100	2.713	100	α-Mn_2O_3; Bixyite;	consists of crystalline α-Mn_2O_3 as a major component, and non-crystalline M_5O_8 as a minor component.
	510	m, sh	509(ii)		1.663	21	1.663	22	JCPDS: 31-0825	
	521	vs	526(i)		3.837	15				
	575	vs	573(i)							
	600	s, sh	607(ii)							
	667	m, sh	668(i)							
MnO_2 (850)	424	w, sh	424(i)	(i) and (ii) as above	2.716	100	2.713	100	α-Mn_2O_3 as above	consists dominantly of crystalline Bixbyite-like α-Mn_2O_3 with trace amounts of non-crystalline Mn_5O_8
	510	w, sh	509(ii)		1.663	22	1.663	22		
	527	vs	526(i)		3.837	16	3.837	15		
	577	vs	573(i)							
	601	m, sh	607(ii)							
	665	m, sh	668(i)							
MnO_2 (1100)	417	m, sh	419	present Mn_3O_4 and	2.475	100	2.480	100	Mn_3O_4; Hausmannite;	consists solely of Hausmannite-like Mn_3O_4

Table 1
(Continued)

	519	vs	517	Hausmannite-like Mn_3O_4 Ref. [18]	2.754	92	2.764	93	JCPDS: 24-0734	$(Mn(II)Mn_2(III)O_4)$
	624	vs	619		1.521	45	1.542	46		
					3.105	44	3.084	44		
MnO_2 (450) H	418	vs	418	present MnO and Manganosite	2.204	100	2.2144	100	MnO; Manganosite;	consists solely of Manganosite-like MnO
	688	w, sh	665	like MnO, Ref. [19]	1.575	60	1.567	58	JCPDS: 7-0230	
					2.499	55	2.558	53		

[a]vw – very weak; w – weak; m – medium; s – strong; vs – very strong; sp – sharp; and sh – shoulder.

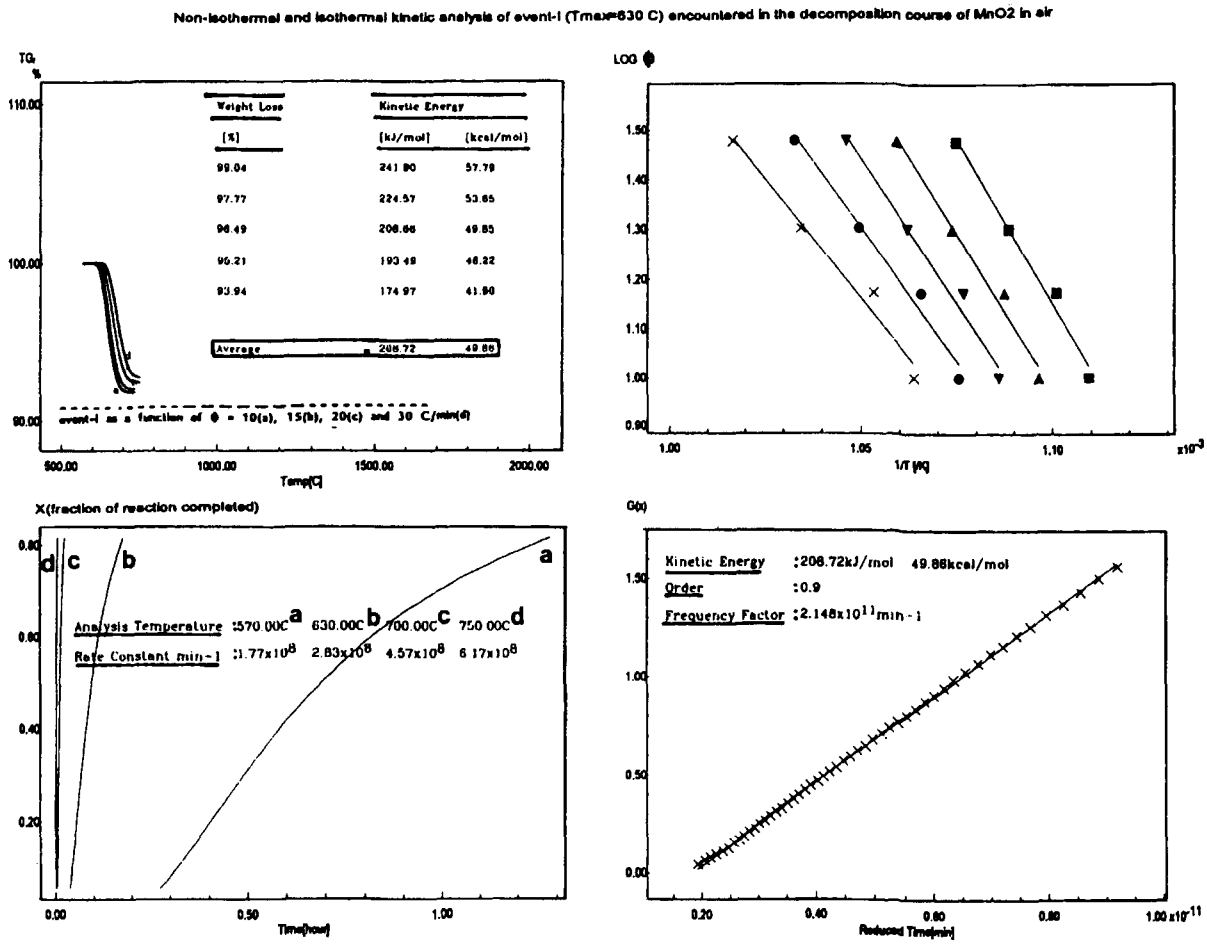

Fig. 2. Non-isothermal and isothermal kinetic analysis of event (I) encountered in the decomposition course of MnO_2 in air (see Fig. 1).

Accordingly, the results confirm reversibility of the redox reaction $3Mn_2O_3 \rightarrow 2Mn_3O_4 + \frac{1}{2}O_2$ and explain the strong dependence of its kinetics on the amount of oxygen in the surrounding atmosphere (Fig. 1 and Table 2).

Looking for a further experimental support to the cyclic TG results, non-cyclic TG was performed on the model Mn-oxides adopted in the present investigation. The curves obtained (Fig. 4) confirm beyond doubt that Mn_3O_4 is the composition responsible for the reversible deoxygenation–oxygenation behaviour montiored in cycle-4 above (Fig. 3). They reveal, moreover, that (i) the oxygenation of Mn_3O_4 is an activation process, since it commences at temperatures no less than 500°C (Fig. 4), and (ii) MnO, the sole product of hydrogen-reduction of MnO_2 at $T_{max} = 450$°C (Fig. 1), also gains weight at 500–1000°C and loses it at > 1000°C (Fig. 4). The weight gain by MnO amounts to ca. 11%. However, the weight loss does not exceed 3%. Hence, these weight changes account for, firstly, oxygenation of MnO to Mn_2O_3 (calc. 11.2%), and secondly, deoxygenation of Mn_2O_3 to Mn_3O_4 (calc. 3.4%). Accordingly, the oxygenation–deoxygenation of MnO appears to be irreversible, in the sense that the deoxygenation does not restore MnO.

Summing up, the results communicated in Figs. 3 and 4 help indicating that the redox component in Mn_3O_4 ($Mn(II)Mn_2(III)O_4$) conversion operates reversibly within the Hausmannite structure assumed

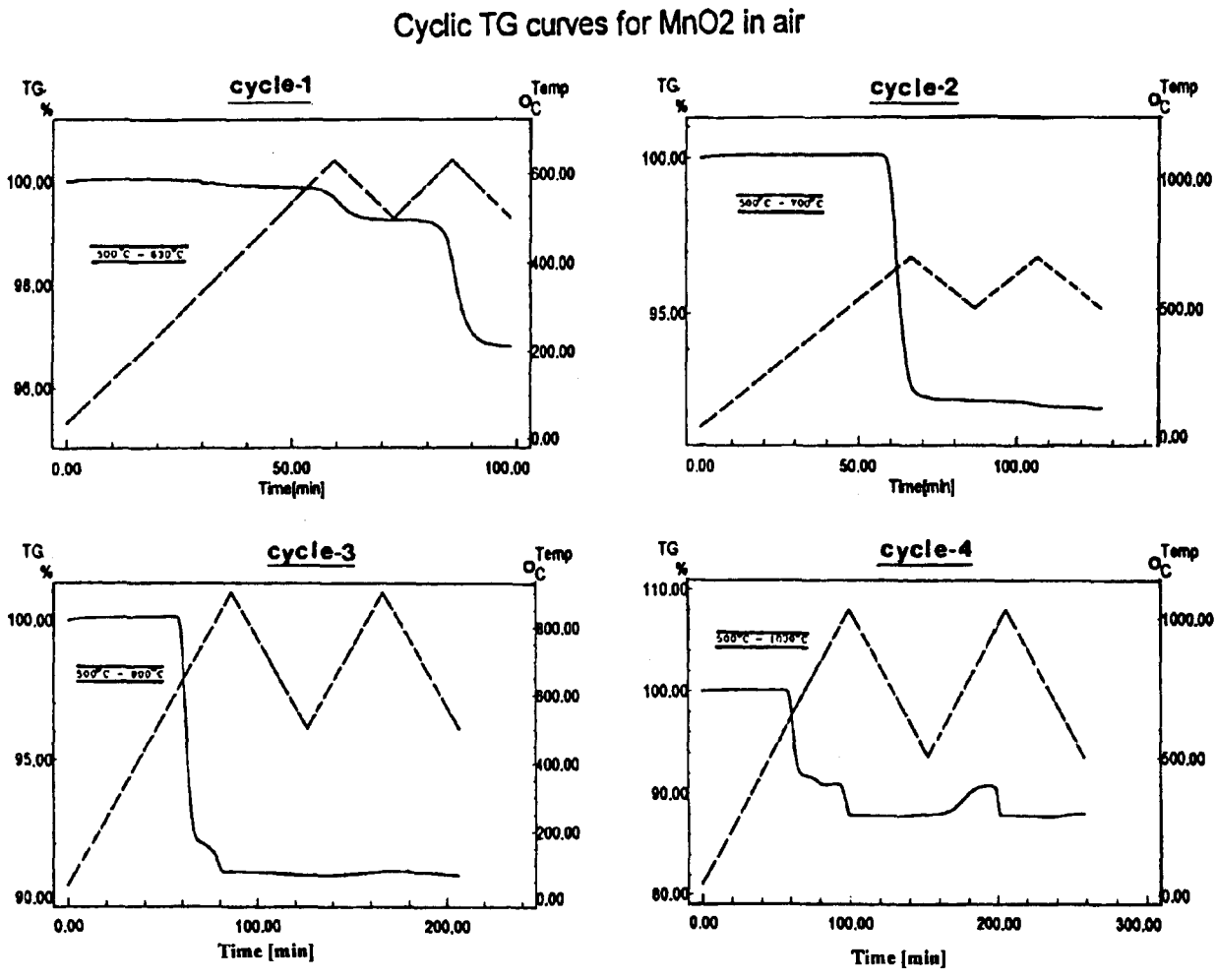

Fig. 3. Cyclic TG curves obtained for MnO_2 in air.

Table 2
Kinetic parameters for thermal events (I and III) observed in the TG of MnO_2 in air (Fig. 1), as derived using Ozawa's method [11]

Event	Activation energy, ΔE/kcal mol^{-1}	Reaction order/n	Frequency factor/A/min^{-1}	Rate constant	
				temperature/(°C)	k/min^{-1}
I	49.96	0.9	2.15×10^{11}	570	1.77×10^{8}
				630	2.83×10^{8}
				700	4.576×10^{8}
				750	6.17×10^{8}
III	128.5	0.6	4.86×10^{21}	970	1.07×10^{15}
				1000	2.64×10^{16}
				1040	3.82×10^{16}

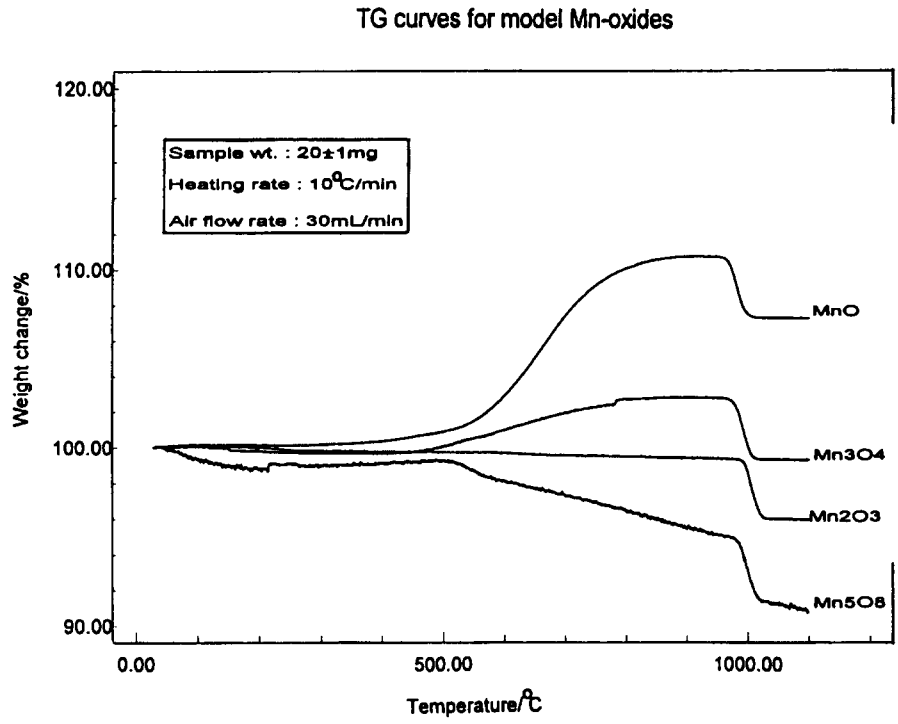

Fig. 4. TG curves obtained in air for the model Mn-oxides indicated.

by the oxide (Table 1). The structural aspect of the process seems to be a key parameter, since the deoxygenation of Mn_2O_3 (the product of MnO oxygenation) is rounded off at the Mn_3O_4 composition instead of going further to restoring MnO. A further emphasis on the structural aspect of the redox behaviour of Mn_3O_4 comes from the fact that Mn_5O_8, a similar Mn(II)-containing mixed oxide composition, does not oxygenate on heating in air (Fig. 4). On the contrary, it deoxygenates gradually to give Mn_2O_3, which, in turn, deoxygenates further at ~1050°C to produce Mn_3O_4 (Fig. 4). Thus, the composition assumed by Mn_5O_8, i.e. $Mn_2(II)Mn_3(IV)O_8$, seems to be incapable of facilitating the appropriate structural requirements for a redox behaviour. An ab initio investigation is being conducted in this laboratory, so as to assess the electron-mobile environment facilitated by Mn(II)/Mn(III) interactions within the structure of Mn_3O_4 vs. Mn(II)/Mn(IV) interactions in the structure of Mn_5O_8.

4. Conclusion

The thermal decomposition of MnO_2 in oxidizing (O_2, air) and non-oxidizing (N_2) gas atmospheres commences at 550°–600°C and results eventually in the formation of Mn_3O_4 at 950°–1050°C. In the reducing atmosphere of H_2, MnO_2 decomposes at 400°–500°C, giving rise to MnO which is stable to further heating in H_2 up to 1050°C. The decomposition course of MnO_2 into Mn_3O_4 is mediated by the formation and decomposition of Mn_5O_8 (at 680°–850°C) and, subsequently, Mn_2O_3 (at 850°–1050°C). In contrast, formation of stable intermediates does not take place in the decomposition course of MnO_2 to MnO (in H_2).

Of the various MnO_x compositions encountered, Mn_3O_4 is the sole composition that tolerates reversible oxygenation–deoxygenation processes at 500°–1050°C: $2Mn_3O_4 + \frac{1}{2}O \rightleftarrows 3Mn_2O_3$. MnO oxygenates at 500°–1050°C giving rise to Mn_2O_3, and deoxygen-

ates subsequently to the onset of formation of Mn_3O_4. Thus, the initial MnO composition is not restored. It is obvious that Mn(II) species formed as a result of a partial deoxygenation of Mn_2O_3 can sustain the remaining Mn(III) species against further deoxygenation, thus resulting in the formation of Mn_3O_4 rather than MnO. An analogous role is played by Mn(II) during the deoxygenation of Mn_5O_8 ($Mn_2(II)Mn_3(IV)O_8$). The product being Mn_2O_3, and not MnO, in a non-reducing atmosphere, indicates a synproportionation of Mn(II)/Mn(IV) to produce Mn(III) species ($= Mn_2O_3$). The electron-mobile environment [1] implied by the redox behaviours of Mn(II)–Mn(IV) and Mn(II)–Mn(III) couples generated in the corresponding mixed-valence MnO_x compositions, i.e. in Mn_5O_8 and Mn_3O_4 respectively, is, according to Sing et al. [20], rather relevant to the redox catalytic conduct of manganese oxides. Consequently, a potential performance of MnO_x-based catalyst in reactions of oxidative coupling of CH_4 [21] has been attributed to the formation of Mn_3O_4-like surface species. Analogously, an active catalytic conduct in deep oxidation reactions [3] can well be anticipated for such MnO_x-based catalysts.

Acknowledgements

The financial support of Kuwait University via projects No. SPC076, SLC056, SLC481–483 and SLG471, and the excellent technical assistance of *Analab* at the Chemistry Department, are highly appreciated.

References

[1] C. Zener, Phys. Rev., 81 (1951) 440; 82 (1951) 403; 83 (1951) 299; and 85 (1952) 324.
[2] B.C. Gates, Catalytic Chemistry, J. Wiley and Sons, Chichester, 1991, pp. 60–62.
[3] R. Prasad, L.A. Kennedy, E. Ruckenstein, Catal. Rev. Sci. Eng., 26 (1984) 1.
[4] P.J. Gellings, H.J.M. Bouwmeester, Catal. Today, 12 (1992) 1.
[5] F. Nakajima, Catal. Today, 10 (1991) 1.
[6] P. Selwood, Adv. Catal., 3 (1951) 27.
[7] G. Gattow, O. Glemser, Z. Anorg. Allg. Chem., 309 (1961) 121.
[8] A.K.H. Nohman, M.I. Zaki, S.A.A. Mansour, R.B. Fahim. C. Kappenstein, Thermochim. Acta, 210 (1992) 103.
[9] M.I. Zaki, A.K.H. Nohman, C. Kappenstein, T.M. Wahdan, J. Mater. Chem., 5 (1995) 1081.
[10] P. Dubois, Compt. Rend., 198 (1934) 1502.
[11] T. Ozawa, Bull. Chem. Soc. Jpn., 38 (1965) 1881.
[12] D.R. Dasgupta, Mineral. Mag., 131 (1965) 135.
[13] M. Sugawara, M. Ohno, K. Matsuki, Chem. Lett., 60 (1991) 1465.
[14] C. Litis, Rev. Chim. Minerale, 4 (1967) 233.
[15] M. le Blanc, G. Wehner, Z. Physik. Chem., A168 (1934) 59.
[16] R.M. Potter, G.R. Rossman, Am. Mineral., 64 (1979) 1199.
[17] W.B. White, V.G. Keramidas, Spectrochim. Acta, 28A (1972) 501.
[18] M. Ishii, M. Nakahira, T. Yamanako, Solid State Commun., 11 (1972) 209.
[19] F. Vratny, M. Dilling, F. Gugliotta, C.N.R. Rao, J. Sci. Ind. Res., 20B (1961) 590.
[20] A. Ellison, J.O.V. Oubridge and K.S.W. Sing, J. Chem. Soc. Faraday Trans, I, 66 (1970) 1004; A. Ellison and K.S.W. Sing, J. Chem. Soc. Faraday Trans. I, 74 (1978) 2807.
[21] G.D. Moggridge, J.P.S. Badyal and R.M. Lambert, J. Phys. Chem., 94 (1990) 508; G.D. Morggridge, T. Rayment and R.M. Lambert, J. Catal., 134 (1992) 242.